CrystEngComm

Accepted Manuscript

ROYAL SOCIETY OF CHEMISTRY

www.rsc.org/crystengcomm

Journal Name RSCPublishing

ARTICLE

A new tactics to achieve $Y_2O_2S:Yb^{3+}/Er^{3+}$ up-conversion luminescent hollow nanofibers

Cite this: DOI: 10.1039/x0xx00000x

Lei Han, Yanhua Hu, Mengmeng Pan, Yangfan Xie, Yangyang Liu, Dan Li, Xiangting Dong*

Received 00th January 2012,
Accepted 00th January 2012

DOI: 10.1039/x0xx00000x

www.rsc.org/

$Y_2O_3:Yb^{3+}/Er^{3+}$ hollow nanofibers were prepared by calcination of the monoaxial electrospinning-made PVP/[$Y(NO_3)_3$+$Yb(NO_3)_3$+$Er(NO_3)_3$] composite nanofibers, and then $Y_2O_2S:Yb^{3+}/Er^{3+}$ hollow nanofibers were synthesized by sulfurization of the as-obtained $Y_2O_3:Yb^{3+}/Er^{3+}$ hollow nanofibers via a double crucible method using sulfur powders as sulfur source. X-ray diffraction (XRD) analysis shows that the $Y_2O_2S:Yb^{3+}/Er^{3+}$ hollow nanofibers are pure hexagonal phase with the space group of $P\bar{3}m1$. Scanning electron microscope (SEM) observation indicates that the $Y_2O_2S:Yb^{3+}/Er^{3+}$ hollow nanofibers are obviously hollow-centered with the mean outer diameter of 226±21 nm. Up-conversion emission spectrum analysis manifests that $Y_2O_2S:Yb^{3+}/Er^{3+}$ hollow nanofibers emit strong green and weak red up-conversion emissions centering at 526, 546 and 667 nm, respectively. The green emissions and the red emission are respectively originated from $^2H_{11/2}/^4S_{3/2}\rightarrow{}^4I_{15/2}$ and $^4F_{9/2}\rightarrow{}^4I_{15/2}$ energy levels transitions of the Er^{3+} ions. The optimum molar ratio of Yb^{3+} to Er^{3+} in $Y_2O_2S:Yb^{3+}/Er^{3+}$ hollow nanofibers is 5:1. The emitting colors of $Y_2O_2S:Yb^{3+}/Er^{3+}$ hollow nanofibers are located in the green region in CIE chromaticity coordinates diagram. The formation mechanism of the $Y_2O_2S:Yb^{3+}/Er^{3+}$ hollow nanofibers is also studied. This preparation technique can be applied to prepare other rare earth oxysulfides hollow nanofibers.

1 Introduction

Up-conversion materials have recently attracted much interest of scientists from various countries due to their special luminescent property[1-3]. In the past a few years, as an important matrix of luminescent materials, Y_2O_2S with high chemical and thermal stability is one of the most important host crystals for lanthanide-doped phosphors[4-5], providing wide band gap (4.6–4.8eV)[6] and suitable Y^{3+} sites where Y^{3+} can be easily substituted by other trivalent rare earth ions without additional charge compensation. Especially, lanthanide ions activated Y_2O_2S have become a very important family of up-conversion materials and have been widely applied in the fields of infrared detection[7], labeling[8-9], and bioimaging[10]. Among the lanthanide ions[11-15], Er^{3+} has attracted much attention as an activator ion owing to its high efficiency property in the up-conversion luminescence[16]. However, the low absorption cross-section of Er^{3+} around 980 nm limits its further commercial applications[17]. Yb^{3+}, having a strong and broad absorption band matching well with the emission wavelength of the laser diode, was reported as an excellent sensitizer for the Er^{3+}-activated optical materials[18-19].

Recently, numerous fabrication methods are reported to fabricate $Y_2O_2S:RE^{3+}$ nanostructures, including solid sate reaction method[20], sol–gel template method[21], flux method[22], combustion method[4], hydrothermal and solvothermal methods[23-25], etc. $Y_2O_2S:RE^{3+}$ materials with different morphologies have been prepared by using the above methods, such as, nanoparticles[26], nanotubes[27], hollow microspheres[28]. However, few reports on preparation of rare earth oxysulfides hollow nanofibers have been found. Hollow nanofibers possess the larger specific surface area compared with their counterpart common solid nanofibers, which is very useful in surface-related applications such as chemical sensors or photocatalysis. Therefore, fabrication of rare earth oxysulfides hollow nanofibers is a meaningful subject of study.

Conventionally, Y_2O_2S nanoparticles are prepared via calcination of the mixture of rare-earth oxides[29-30] or oxalate compounds[31-32] or carbonates[33-34], sulfur powders and flux (Na_2CO_3, $Mg_2CO_3{\cdot}4Mg(OH)_2{\cdot}5H_2O$, TiO_2) at elevated temperatures. In this way, the as-prepared nanoparticles often have irregular morphology and cannot inherit the peculiar morphologies of rare earth oxides precursors because sulfur powders will melt and destruct the morphologies of rare earth oxides. Hence, it is difficult to obtain rare earth oxysulfides hollow nanofibers via direct solid-state reaction using rare earth oxides hollow nanofibers as precursors. In order to solve this problem, a double-crucible method is used for succeeding to the morphology of the $Y_2O_3:RE^{3+}$ hollow nanofibers used as precursors, and it is expected that unbroken $Y_2O_2S:RE^{3+}$ hollow nanofibers will be obtained.

Electrospinning is a simple and effective method to fabricate one-dimensional micro- and nanomaterials[35-38]. PVP has been widely used for electrospinning owing to its good solubility, high flexibility, non-toxicity, easy obtainment, low costs, etc[39-40]. By using PVP as template via electrospinning technique, one-dimensional nanomaterials with various morphologies have been successfully prepared, such as nanofibers[41], nanocable[42], core-shell structured coaxial nanofibers[43], nanobelts[44-45]. However, to the best of our knowledge, there have been no reports on the preparation of rare earth oxysulfides hollow nanofibers by electrospinning combined with sulfurization technique in the literatures. In this paper, $Y_2O_3:Yb^{3+}/Er^{3+}$ hollow nanofibers were

fabricated via calcination of the electrospun PVP/[$Y(NO_3)_3$+$Yb(NO_3)_3$+$Er(NO_3)_3$] composite nanofibers at 700 ºC, and then Y_2O_2S:Yb^{3+}/Er^{3+} hollow nanofibers were synthesized by sulfurization of the as-prepared Y_2O_3:Yb^{3+}/Er^{3+} hollow nanofibers via a double crucible sulfurization method. The samples were systematically characterized, and some meaningful results were obtained.

2 Experimental Section

2.1 Chemicals

Polyvinyl pyrrolidone (PVP; K15, $M_w \approx 10{,}000$, AR) was bought from Tiantai Chemical Co., Ltd. Erbium oxide (Er_2O_3, 99.99 %), ytterbium oxide (Yb_2O_3, 99.99 %) and yttrium oxide (Y_2O_3, 99.99 %) were purchased from Kemiou Chemical Co., Ltd. N, N-dimethylformamide (DMF, AR) was purchased from Sinopharm Chemical Reagent Co., Ltd. Nitric acid (HNO_3, AR) was purchased from Beijing Chemical Works. All chemicals were directly used as received without further purification.

2.2 Synthesis of Y_2O_3:Yb^{3+}/Er^{3+} hollow nanofibers

In the typical procedure of preparing representative Y_2O_3:10%Yb^{3+}/2%Er^{3+} hollow nanofibers, 0.8370 g of yttrium oxide, 0.0322 g of erbium oxide and 0.1660 g of ytterbium oxide were dissolved in dilute nitric acid at elevated temperatures and evaporated by heating to obtain the mixture of $Y(NO_3)_3\cdot 6H_2O$, $Er(NO_3)_3\cdot 6H_2O$ and $Yb(NO_3)_3\cdot 6H_2O$ powders. Then the mixture of rare earth nitrates was dissolved in 9.8000 g of DMF, and then 7.8000 g of PVP was added into the above solution under magnetic stirring for 8 h to form homogeneous transparent spinning solution. In the spinning solution, the mass ratios of rare earth nitrates, PVP and DMF were equal to 12:39:49. Subsequently, the spinning solution was electrospun using a traditional single-spinneret electrospinning setup at room temperature under a positive high voltage of 16 kV, the distance between the spinneret and the collector was fixed to 18 cm, and relative humidity was 30 %-60 %. With the evaporation of DMF, PVP/[$Y(NO_3)_3$+$Yb(NO_3)_3$+$Er(NO_3)_3$] composite nanofibers were collected on the collector. Then, Y_2O_3:10%Yb^{3+}/2%Er^{3+} hollow nanofibers were obtained by calcining as-prepared PVP/[$Y(NO_3)_3$+$Yb(NO_3)_3$+$Er(NO_3)_3$] composite fibers at 700 ºC for 8 h with a heating rate of 1 ºC·min^{-1} in air. Other series of Y_2O_3:10%Yb^{3+}/x%Er^{3+} (x = 0.5, 1 and 3) hollow nanofibers were prepared by the similar procedures except for different doping molar concentration of Er^{3+} ions.

2.3 Fabrication of Y_2O_2S:Yb^{3+}/Er^{3+} hollow nanofibers

The as-obtained Y_2O_3:10%Yb^{3+}/x%Er^{3+} (x = 0.5, 1, 2 and 3) hollow nanofibers were sulfurated by using a double crucible method. The process of the double crucible method was as follows: some sulfur powders were put into a small crucible, and carbon rods were loaded on the sulfur powders, Y_2O_3:Yb^{3+}/Er^{3+} hollow nanofibers were loaded on the carbon rods, then the small crucible was placed into a large crucible, and excess sulfur powders were added into the space between the two crucibles, and then the large crucible was covered with its lid. The crucibles were annealed at 800 °C for 4 h with a heating rate of 5 ºC·min^{-1} under argon atmosphere, then the temperature was decreased to 200 °C at a rate of 5 ºC·min^{-1}, followed by naturally down to room temperature. Thus, Y_2O_2S:Yb^{3+}/Er^{3+} hollow nanofibers were acquired.

3 Characterization

The scanning electron microscope (FESEM, XL-30 ESEM FEG Micro FEI Philips) was used to characterize the morphologies of the products. Energy dispersive X-ray spectrometer attached to scanning electron microscope (SEM) was employed to analyze the composition of samples. X-ray diffraction (XRD) analysis was performed using a Rigaku D/max-RA X-ray diffractometer with Cu Kα line of 0.15418 nm. The operation voltage and current were kept at 30 kV and 20 mA, respectively. The up-conversion luminescent spectra were determined with a Hitachi F-4500 fluorescent spectrometer using a power-tunable 980-nm diode laser. The histograms of diameters were drawn by Image-Pro-Plus 6.0 and origin 8.5 softwares.

4 Results and Discussion

4.1 XRD analysis

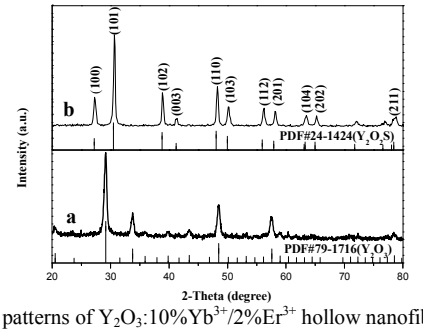

Fig. 1 XRD patterns of Y_2O_3:10%Yb^{3+}/2%Er^{3+} hollow nanofibers (a) and Y_2O_2S:10%Yb^{3+}/2%Er^{3+} hollow nanofibers (b) with PDF standard cards of Y_2O_3 and Y_2O_2S

Fig. 1 shows the XRD patterns of Y_2O_3:Yb^{3+}/Er^{3+} hollow nanofibers and Y_2O_2S:Yb^{3+}/Er^{3+} hollow nanofibers. It can be seen that diffraction peaks of Y_2O_3:Yb^{3+}/Er^{3+} hollow nanofibers can be readily indexed to those of the pure cubic phase with primitive structure of Y_2O_3 (PDF#79-1716). The XRD analysis of Y_2O_2S:Yb^{3+}/Er^{3+} hollow nanofibers reveals that the diffraction peaks can be easily indexed to those of the pure hexagonal phase with primitive structure of Y_2O_2S (PDF#24-1424), and the space group is $P\bar{3}m1$. Obvious diffraction peaks for Y_2O_2S:Yb^{3+}/Er^{3+} are located near 2θ=27.25°(100), 30.625°(101), 38.875°(102), 41.25°(003), 48.25°(110), 50.12°(103), 56.12°(112), 58.12°(201), 63.62°(104), 65.25°(202), 78.75°(211), etc. No peaks of any other phases or impurities are detected, indicating crystalline Y_2O_2S:Yb^{3+}/Er^{3+} with pure phase were successfully obtained.

4.2 SEM analysis

Fig. 2 demonstrates the morphologies of Y_2O_3:Yb^{3+}/Er^{3+} hollow nanofibers and Y_2O_2S:Yb^{3+}/Er^{3+} hollow nanofibers. It can be clearly seen that the morphology of fibers is hollow-centered structure, and hollow nanofibers have good dispersion and uniform size distribution. In order to investigate the diameter distribution of the samples, Image-Pro Plus 6.0 software is used to measure diameters of 100 hollow nanofibers from SEM images, and the results are analyzed with statistics, as indicated in Fig. 3. The diameters of Y_2O_3:Yb^{3+}/Er^{3+} hollow nanofibers and Y_2O_2S:Yb^{3+}/Er^{3+} hollow nanofibers are respectively 216±11 nm and 226±21 nm under the 95 % confidence level.

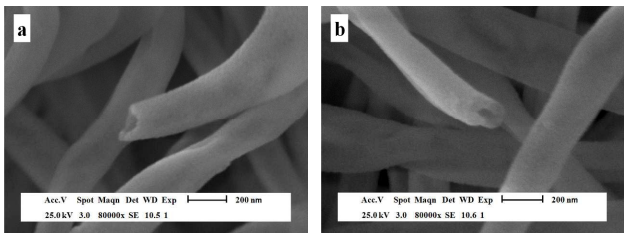

Fig. 2 SEM images of Y_2O_3:10%Yb^{3+}/2%Er^{3+} hollow nanofibers (a) and Y_2O_2S:10%Yb^{3+}/2%Er^{3+} hollow nanofibers (b)

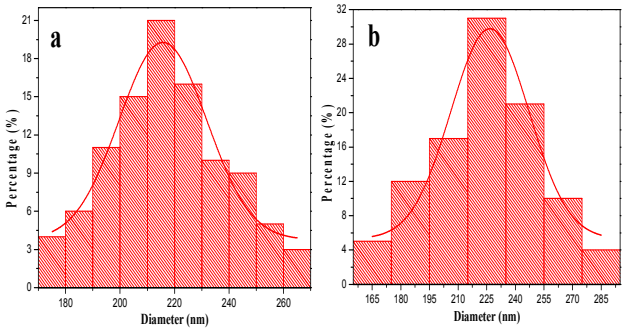

Fig. 3 Histograms of diameters distribution of Y_2O_3:10%Yb^{3+}/2%Er^{3+} (a) and Y_2O_2S:10%Yb^{3+}/2%Er^{3+} (b) hollow nanofibers

4.3 Energy dispersive spectrum analysis

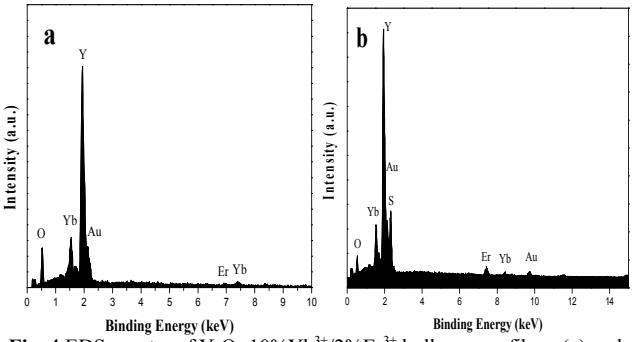

Fig. 4 EDS spectra of Y_2O_3:10%Yb^{3+}/2%Er^{3+} hollow nanofibers (a) and Y_2O_2S:10%Yb^{3+}/2% Er^{3+} hollow nanofibers (b)

Fig. 4 shows the EDS spectra of Y_2O_3:Yb^{3+}/Er^{3+} hollow nanofibers and Y_2O_2S:Yb^{3+}/Er^{3+} hollow nanofibers. The presence of Y, O, Yb, Er elements for the Y_2O_3:Yb^{3+}/Er^{3+} hollow nanofibers and the presence of Y, O, S, Yb, Er elements for the Y_2O_2S:Yb^{3+}/Er^{3+} hollow nanofibers indicate that highly pure Y_2O_3:Yb^{3+}/Er^{3+} hollow nanofibers and Y_2O_2S:Yb^{3+}/Er^{3+} hollow nanofibers are obtained. Au peak is from the conductive film of Au plated on the sample for SEM observation.

4.4 Up-conversion luminescence properties

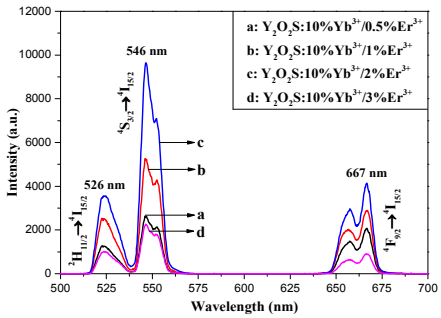

Fig. 5 Up-conversion emission spectra of Y_2O_2S:10%Yb^{3+}/x%Er^{3+} (x = 0.5, 1, 2, 3) hollow nanofibers excited at 980-nm diode laser

Fig. 5 shows the up-conversion emission spectra (excited by a 980-nm diode laser) of Y_2O_2S:10%Yb^{3+}/x%Er^{3+} (x = 0.5, 1, 2, 3) hollow nanofibers under the pump power of 157 mW. One can see that the hollow nanofibers emit strong green and weak red up-conversion emissions centering at 526, 546 and 667 nm, respectively. The strong green emissions belong to the $^2H_{11/2}\rightarrow{}^4I_{15/2}$ (526 nm) and $^4S_{3/2}\rightarrow{}^4I_{15/2}$ (546 nm) energy levels transitions of Er^{3+} ions, and the weak red emission is assigned to the transition of $^4F_{9/2}\rightarrow{}^4I_{15/2}$ (667 nm) energy levels of Er^{3+} ions. The peak positions and spectral shapes of emission spectra are not influenced by Yb^{3+} and Er^{3+} concentration. Obviously, the luminescence intensity of Y_2O_2S:10%Yb^{3+}/x%Er^{3+} (x = 0.5, 1, 2, 3) hollow nanofibers increases with the increase of the concentration of Er^{3+} ions from the beginning, and reaches a maximum value with the Er^{3+} concentration of 2 %, and then decrease with the further increase in Er^{3+} concentration. Therefore, the optimum molar ratio of Yb^{3+} to Er^{3+} in Y_2O_2S:Yb^{3+}/Er^{3+} hollow nanofibers is 5:1.

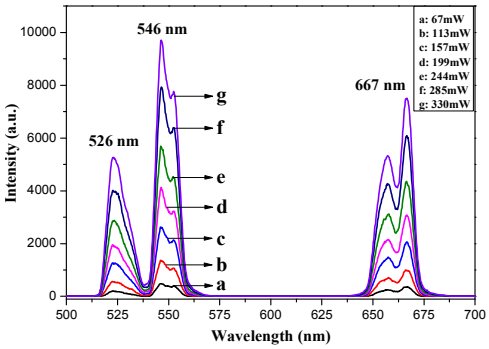

Fig. 6 Up-conversion emission spectra of Y_2O_2S:10%Yb^{3+}/0.5%Er^{3+} hollow nanofibers under the excitation of a 980-nm diode laser with different pump powers

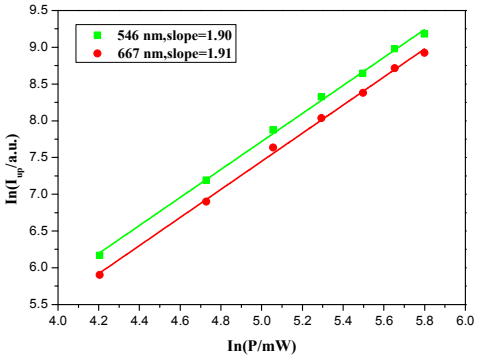

Fig. 7 Plots of natural logarithm intensity of the up-conversion emissions (I_{up}) versus natural logarithm pumped power of diode laser (P) for Y_2O_2S:10%Yb^{3+}/0.5%Er^{3+} hollow nanofibers

The up-conversion emission spectra of Y_2O_2S:10%Yb^{3+}/0.5%Er^{3+} hollow nanofibers under the excitation of a 980-nm diode laser with different pump powers are indicated in Fig. 6. It is seen that the up-conversion luminescence intensity of Y_2O_2S:10%Yb^{3+}/0.5%Er^{3+} hollow nanofibers increases with the increase of pump powers. The study has been shown that the visible output power intensity (I_{up}) is proportional to the infrared excitation power (P)[46]:

$$I_{up} \propto P^n \qquad (1)$$

Where n is the number of IR photons absorbed per visible phonon emitted. Fig. 7 reveals the natural logarithm plots of the emission

intensity as a function of pump power for the green (546 nm) and red (667 nm) emissions in Y_2O_2S:10%Yb^{3+}/0.5%Er^{3+} hollow nanofibers with different powers, respectively. For the green and red emissions, the values of n (the slope) are determined to be 1.90 and 1.91, respectively. Generally, a straight line with the slope approximate 2 for the up-conversion luminescence indicates two photons involve in this up-conversion luminescence process. From the above result, it has been proved that the green and red emissions of $Y_2O_2S:Yb^{3+}/Er^{3+}$ hollow nanofibers are all two photons process.

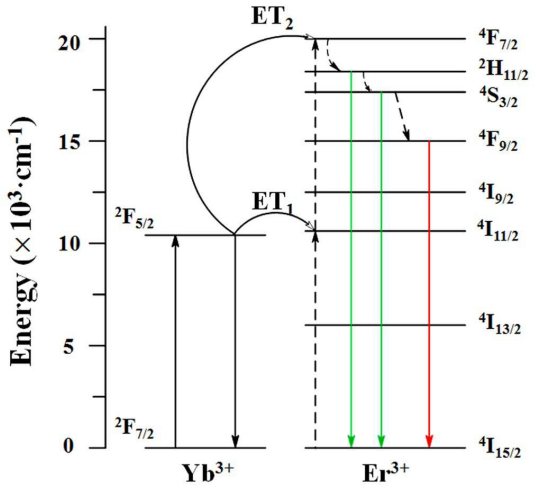

Fig. 8 Up-conversion luminescent mechanism and population processes in Er^{3+} and Yb^{3+} co-doped systems

In principle, four basic population mechanisms may be involved in the UC process, namely energy transfer (ET), ground state absorption (GSA), excited state absorption (ESA) and photo avalanche (PA).[47] We can immediately rule out PA as a mechanism of up-conversion in $Y_2O_2S:Yb^{3+}/Er^{3+}$ hollow nanofibers because no inflection point is observed in the power study. The up-conversion luminescence mechanism and processes in Er^{3+} and Yb^{3+} co-doped materials are shown in Fig. 8. The green and red efficient up-conversion occur via the two-step energy transfer (ET) from the excited Yb^{3+} to Er^{3+} and little contribution from Er^{3+} ground/excited state absorption (GSA/ESA). At first, Yb^{3+} ions are excited from $^2F_{7/2}$ to $^2F_{5/2}$ level by 980-nm laser, and then the Er^{3+} ions are excited from the ground state $^4I_{15/2}$ to the excited state $^4I_{11/2}$ via ET of neighboring Yb^{3+} [$^4I_{15/2}$ (Er)+$^2F_{5/2}$ (Yb)→$^4I_{11/2}$ (Er)+$^2F_{7/2}$ (Yb)]. Then, nonradiative relaxations of $^4I_{11/2}$→$^4I_{13/2}$ also populate the $^4I_{13/2}$ energy level. Following this process, immediate energy transfer from another excited Yb^{3+} ion to Er^{3+} ion results in population of the $^4F_{7/2}$ state. Subsequently, the excited ions on $^4F_{7/2}$ nonradiatively relax to the green levels of $^4S_{3/2}$ and $^2H_{11/2}$, which results in the observed emission spectra, namely, 526 and 546 nm corresponding to green emission of $^2H_{11/2}/^4S_{3/2}$→$^4I_{15/2}$, and 667 nm corresponding to red emission of $^4F_{9/2}$→$^4I_{15/2}$ of Er^{3+}.[48]

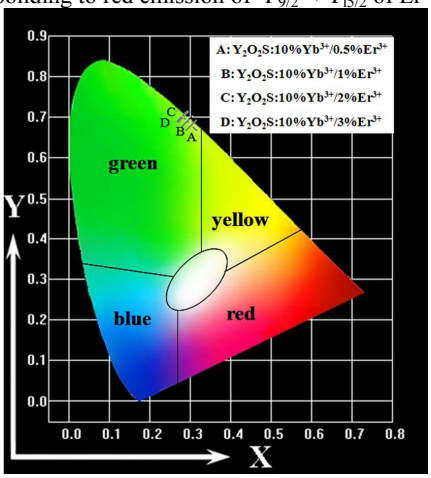

Fig. 9 CIE chromaticity coordinates diagram of Y_2O_2S:10%Yb^{3+}/x%Er^{3+} (x=0.5, 1, 2, 3) hollow nanofibers

Generally, color can be represented by the Commission International del'Eclairage (CIE) 1931 chromaticity coordinates. The color coordinates for the green emission in the present experiment are calculated based on the corresponding up-conversion emission spectra and the results are shown in Fig. 9. All of samples are located in the green light area, the coordinates of Y_2O_2S:10%Yb^{3+}/x%Er^{3+} (x=0.5, 1, 2, 3) hollow nanofibers are (0.303, 0.679), (0.292, 0.69), (0.281, 0.702) and (0.273, 0.708), which are respectively corresponded to the Er^{3+} ion concentration of 0.5, 1, 2 and 3 %. Based on the above analysis, it is obviously found that the emission colors of $Y_2O_2S:Yb^{3+}/Er^{3+}$ hollow nanofibers are tunable by changing the concentration of doping Er^{3+} ions.

4.5 Formation mechanism for $Y_2O_2S:Yb^{3+}/Er^{3+}$ hollow nanofibers

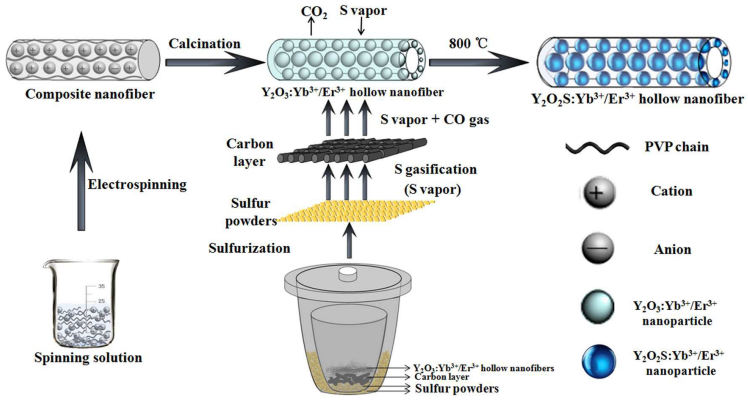

Fig. 10 Formation mechanism of $Y_2O_2S:Yb^{3+}/Er^{3+}$ hollow nanofibers

Fig. 10 shows the formation mechanism of $Y_2O_2S:Yb^{3+}/Er^{3+}$ hollow nanofibers. PVP, $Y(NO_3)_3$, $Yb(NO_3)_3$ and $Er(NO_3)_3$ were mixed with DMF to form spinning solution. Y^{3+}, Yb^{3+}, Er^{3+} and NO_3^- were mixed or absorbed onto PVP to form sol with certain

viscosity, and then PVP/[$Y(NO_3)_3$+$Yb(NO_3)_3$+$Er(NO_3)_3$] composite nanofibers were fabricated via electrospinning of the spinning solution. During the calcination process, PVP chain was broken and volatilized. The Y^{3+}, Yb^{3+}, Er^{3+} and NO_3^- ions were diffused to the surface of composite fibers along with the evaporation of solvent DMF. With the increase in calcination temperature, nitrate was decomposed and oxidized to NO_2, Y^{3+}, Yb^{3+} and Er^{3+} were oxidized to form Y_2O_3:Yb^{3+}/Er^{3+} crystallites, many crystallites were combined into nanoparticles, then some nanoparticles were mutually connected to generate hollow-centered Y_2O_3:Yb^{3+}/Er^{3+} nanofibers. PVP acted as template during the formation of Y_2O_3:Yb^{3+}/Er^{3+} hollow nanofibers.

In the sulfurization process, Y_2O_3:Yb^{3+}/Er^{3+} hollow nanofibers were sulfurized using S as a sulfurization agent and S was gasified at about 350 °C. With the increase of calcination temperature, gasified sulfur reacts with Y_2O_3:Yb^{3+}/Er^{3+} hollow nanofibers to produce Y_2O_2S:Yb^{3+}/Er^{3+} hollow nanofibers. During reaction process, sulfur powders and Y_2O_3:Yb^{3+}/Er^{3+} hollow nanofibers were separated by carbon rods which prevented Y_2O_3:Yb^{3+}/Er^{3+} hollow nanofibers from morphology damage and also played a key role in reduction through reacting with oxygen species of Y_2O_3:Yb^{3+}/Er^{3+} in the heating process. The double-crucible method we proposed here is actually a solid-gas reaction, which has been proved to be an important method, not only can retain the morphology of the Y_2O_3:Yb^{3+}/Er^{3+} hollow nanofibers, but also can fabricate the Y_2O_2S:Yb^{3+}/Er^{3+} hollow nanofibers with pure phase at relatively low temperature. Reaction schemes for the formation of the Y_2O_2S:Yb^{3+}/Er^{3+} hollow nanofibers proceed as follows:

$$PVP[Y(NO_3)_3+Yb(NO_3)_3+Er(NO_3)_3]+O_2 \xrightarrow{700\ ^oC} CO_2+H_2O+NO_2+Y_2O_3:Yb^{3+}/Er^{3+}\ (1)$$

$$Y_2O_3:Yb^{3+}/Er^{3+}+C+S \xrightarrow{800\ ^oC} Y_2O_2S:Yb^{3+}/Er^{3+}+CO\ (2)$$

$$Y_2O_3:Yb^{3+}/Er^{3+}+S+CO \xrightarrow{800\ ^oC} Y_2O_2S:Yb^{3+}/Er^{3+}+CO_2\ (3)$$

5 Conclusions

Y_2O_2S:Yb^{3+}/Er^{3+} hollow nanofibers have been fabricated via sulfurization of electrospinning-derived Y_2O_3:Yb^{3+}/Er^{3+} hollow nanofibers by using a double-crucible method. Y_2O_2S:Yb^{3+}/Er^{3+} hollow nanofibers are pure hexagonal phase with space group of $P\bar{3}m1$. The morphology of fibers is hollow-centered structure and the mean outer diameter of hollow nanofibers is 226±21 nm. Y_2O_2S:Yb^{3+}/Er^{3+} hollow nanofibers emit strong green and weak red up-conversion emissions centering at 526, 546 and 667 nm belonged to the $^2H_{11/2}\rightarrow{}^4I_{15/2}$, $^4S_{3/2}\rightarrow{}^4I_{15/2}$ and $^4F_{9/2}\rightarrow{}^4I_{15/2}$ energy levels transition of Er^{3+} ion, respectively. The optimum molar ratio of Yb^{3+} to Er^{3+} in Y_2O_2S:Yb^{3+}/Er^{3+} hollow nanofibers is 5:1. The emission colors of Y_2O_2S:Yb^{3+}/Er^{3+} hollow nanofibers are tunable by changing the concentration of doping Er^{3+} ions. The formation mechanism of Y_2O_2S:Yb^{3+}/Er^{3+} hollow nanofibers is also proposed. The present work provides a new route to fabricate hollow nanofibers of rare earth oxysulfides.

Acknowledgments

This work was financially supported by the National Natural Science Foundation of China (NSFC 50972020, 51072026), Specialized Research Fund for the Doctoral Program of Higher Education (20102216110002, 20112216120003), the Science and Technology Development Planning Project of Jilin Province (Grant Nos. 20130101001JC, 20070402), the Science and Technology Research Project of the Education Department of Jilin Province during the eleventh five-year plan period(Under grant No. 2010JYT01)

Notes and references

Key Laboratory of Applied Chemistry and Nanotechnology at Universities of Jilin Province, Changchun University of Science and Technology, Changchun 130022. Fax: 86 0431 85383815; Tel: 86 0431 85582574; E-mail: dongxiangting888@163.com

1 G. Y. Chen, H. L. Qiu, P. N. Prasad and X. Y. Chen, *Chem. Rev.*, 2014, **114(10)**, 5161-5214.
2 S. Wang, S. Q. Su, S. Y. Song, R. P. Deng and H. J. Zhang, *CrystEngComm*, 2012, **14**, 4266-4269.
3 S. Wang, S. Y. Song, R. P. Deng, H. L. Guo, Y. Q. Lei, F. Cao, X. Y. Li, S. Q. Su and H. J. Zhang, *CrystEngComm*, 2010, **12**, 3537-3541.
4 Y. J. Li, M. W. Wang, L. D. Zhang, D. Gao and S. X. Liu, *Int. J. Min. Met. Mater.*, 2013, **20(10)**, 972-977.
5 O. Y. Manashirov, A. N. Georgobiani, V. B. Gutan, E. M. Zvereva and A. N. Lobanov, *Inorg. Mater.*, 2012, **48(7)**, 721-726.
6 M. Mikami and A. Oshiyama, *Phys. Rev. B.*, 1998, **57(15)**, 8939-8944.
7 P. L. A. M. Corstjens, S. Li, M. Zuiderwijk, K. Kardos, W. R. Abrams, R. S. Niedbala and H. J. Tanke, *IEE P- Nanobiotechnol*, 2005, **152(2)**, 64-72.
8 F. Wang, W. B. Tan, Y. Zhang, X. Fan and M. Wang, *Nanotechnology*, 2006, **17(1)**, R1-R13.
9 G. Cheng, J. L. Zhang, Y. L. Liu, D. H. Sun and J. Z. Ni, *Chem. Commun.*, 2011, **47(20)**, 5732-5734.
10 S. Santra, J. Xu, K. Wang and W. Tand, *J. Nanosci. Nanotechnol*, **2004, 4(6)**, 590-599.
11 X. H. Yin, Q. Zhao, B. Q. Shao, W. Lv, Y. H. Li and H. P. You, *CrystEngComm*, 2014, **16(25)**, 5543-5550.
12 M. Yang, H. P. You, N. Guo, Y. J. Huang, Y. H. Zheng and H. J. Zhang, *CrystEngComm*, 2010, **12**, 4141-4145.
13 L. Kong, S. C. Gan, G. Y. Hong, H. P. You and J. L. Zhang, *Chem. J. Chinese U.*, 2008, **29(4)**, 673-676.
14 G. Jia, G. M. Zhang, S. W. Ding, L. Y. Wang, L. F. Li and H. P. You, *CrystEngComm*, 2012, **14**, 573-578.
15 Q. Zhao, Y. H. Zheng, N. Guo, Y. C. Jia, H. Qiao, W. Z. Lv and H. P. You, *CrystEngComm*, 2012, **14**, 6659-6664.
16 J. Yang, C. X. Li, Z. W. Quan, C. M. Zhang, P. P. Yang, Y. Y. Li, C. C. Yu and J. Lin, *J. Phys. Chem. C*, 2008, **112(33)**, 12777-12785.
17 D. Li, X. T. Dong, W. S. Yu, J. X. Wang, and G. X. Liu, *J. Nanopart. Res.*, 2013, **15(6)**, 1-10.
18 G. Jia, H. P. You, Y. H. Zheng, K. Liu, N. Guo and H. J. Zhang, *CrystEngComm*, 2010, **12(10)**, 2943-2948.
19 Y. Wu, D. M. Yang, X. J. Kang, Y. Zhang, S. S. Huang, C. Li and J. Lin, *CrystEngComm*, 2014, **16**, 1056-1063.
20 P. Jiao, *New chem. Mat.*, 2014, **42(5)**, 65-67.
21 C. E. Cui, H. Liu, P. Huang and L. Wang, *J. Lumin*, 2014, **149**, 196-199.
22 P. D. Han, L. Zhang, Y. Chen, L. X. Wang and Q. T. Zhang, *Mater. Sci. Forum*, 2011, **663**, 381-384.
23 D. Liu, P. Huang, C. E. Cui, L. Wang and G. W. Jiang, *Ceram. Int.*, 2014, **40**, 117-122.
24 H. Chen, Y. C. Zhang, C. Chen, Z. L. Wang and N. Yao, *Appl. Mech. Mater.*, 2014, **513**, 138-142.
25 J. Thirumalai, R. Chandramohan, S. Valanarasu, T. A. Vijayan and S. Ezhilvizhian, *Micro Nano Lett.*, 2011, **6(8)**, 614-618.
26 T. Pang, W. H. Cao, M. M. Xing, W. Feng, S. J. Xu and X. X. Luo, *J. Rare Earth*, 2010, **28(4)**, 509-512.
27 C. E. Cui, G. W. Jiang, P. Huang, L. Wang and D. Liu, *Ceram. Int.*, 2014, **40(3)**, 4725-4730.
28 S. Q. Deng, Z. P. Xue, Y. L. Liu, B. F. Lei, Y. Xiao and M. T. Zheng, *J. Alloys Compd.*, 2012, **542**, 207-212.
29 Y. Y. Li, S. H. Cai and D. C. Dai, *J. Rare Earth*, 1996, **14(4)**, 275-278.
30 H. G. Kim, D. W. Hwang and J. S. Lee, *J. Amer. Chem. Soc.*, 2004, **126(29)**, 8912-8913.
31 F. Wang, B. Yang, J. C. Zhang, Y. N. Dai and W. H. Ma, *J. Lumin.*, 2010, **130(3)**, 473-477.

32 A. M. Pires, O. A. Serra and M. R. Davolos, *J. Alloys Compd.*, 2004, **374(1)**, 181-184.
33 P. F. Ai, W. Y. Li, L. Y. Xiao, Y. D. Li, H. J. Wang and Y. L. Liu, *Ceram. Int.*, 2010, **36(7)**, 2169-2174.
34 Y. Fu, W. H. Cao, Y. Peng, X. X. Luo and M. M. Xing, *J. Mater. Sci.*, 2010, **45(23)**, 6556-6561.
35 Q. L. Ma, J. X. Wang, X. T. Dong, W. S. Yu and G. X. Liu, *RSC Adv.*, 2015, **5(4)**, 2523-2530.
36 X. Peng, A. C. Santulli, E. Sutter, S. S. Wong, *Chem. Sci.*, 2012, **3(4)**, 1262-1272.
37 Q. L. Ma, W. S. Yu, X. T. Dong, J. X. Wang and G. X. Liu, *Nanoscale*, 2014, **6(5)**, 2945-2952.
38 Q. L. Ma, J. X. Wang, X. T. Dong, W. S. Yu and G. X. Liu, *ChemPlusChem*, 2014, **79(2)**, 290-297.
39 S. J. Sheng, Q. L. Ma, X. T. Dong, N. Lv, J. X. Wang, W. S. Yu and G. X. Liu, *J. Mater. Sci.: Mater. El.*, 2014, **25**, 2279-2286.
40 N. Lv, Q. L. Ma, X. T. Dong, J. X. Wang, W. S. Yu and G. X. Liu, *ChemPlusChem*, 2014, 79, 690-697.
41 W. W. Pan, R. Han, X. Chi, Q. F. Liu and J. B. Wang, *J. Alloys Compd.*, 2013, **577**, 192-194.
42 Z. Y. Zhang, C. L. Shao, Y. Y. Sun, J. B. Mu, M. Y. Zhang, P. Zhang, Z. C. Guo, P. P. Liang, C. H. Wang and Y. C. Liu, *J. Mater. Chem.*, 2012, **22(4)**, 1387-1395.
43 Q. L. Ma, J. X. Wang, X. T. Dong, W. S. Yu and G. X. Liu, *J. Nanopart. Res.*, 2014, **16(2)**, 2239-2248.
44 X. M. Guo, J. X. Wang, X. T. Dong, W. S. Yu and G. X. Liu, *CrystEngComm*, 2014, **16(24)**, 5409-5417
45 W. W. Ma, X. T. Dong, J. X. Wang, W. S. Yu and G. X. Liu, *J. Electron. Mater.*, 2014, **43(9)**, 3701-3707.
46 G. S. Yi, B. Q. Sun, F. Z. Yang, D. P. Chen, Y. X. Zhou and J. Cheng, *Chem. Mater.*, 2002, **14(7)**, 2910-2914.
47 W. W. Ma, W. S. Yu , X. T. Dong, J. X. Wang and G. X. Liu, *Lumin.*, 2014, **29(7)**, 908–913.
48 Y. H. Song, Y. J. Huang, L. H. Zhang, Y. H. Zheng, N. Guo and H. P. You, *RSC Adv.*, 2012, **2**, 4777-4781.

Revised Graphical Abstract

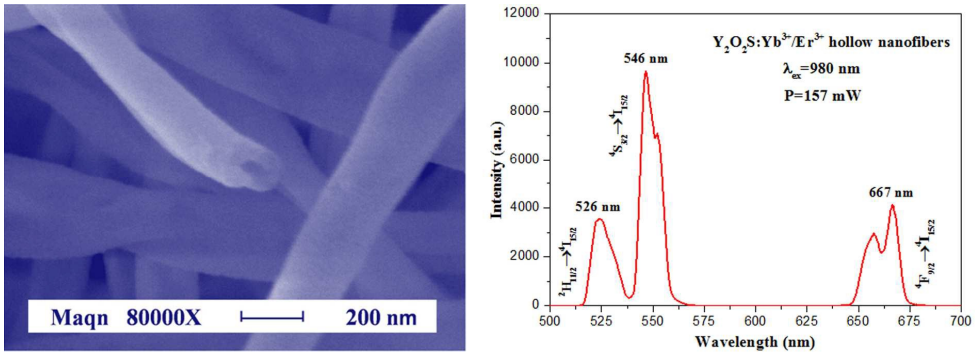

$Y_2O_2S:Yb^{3+}/Er^{3+}$ hollow nanofibers were synthesized via inheriting morphology of electrospinning-derived precursor and exhibit excellent up-conversion luminescence properties.